DSTN hypomethylation promotes radiotherapy resistance of rectal cancer by activating Wnt/β-catenin signaling pathway

Rongbo Wen
Changhai Hospital, Naval Medical University
Leqi Zhou
Changhai Hospital, Naval Medical University
Siyuan Jiang
Changhai Hospital, Naval Medical University
Hao Fan
Changhai Hospital, Naval Medical University
Kuo Zheng
Changhai Hospital, Naval Medical University
Yue Yu
Changhai Hospital, Naval Medical University
Xianhua Gao
Changhai Hospital, Naval Medical University
Liqiang Hao
Changhai Hospital, Naval Medical University
Zheng Lou
Changhai Hospital, Naval Medical University
Guanyu Yu
Changhai Hospital, Naval Medical University
Fu Yang
Naval Medical University
Wei Zhang (weizhang2000cn@163.com)
Changhai Hospital, Naval Medical University

Research Article

Keywords: rectal cancer, neoadjuvant radiotherapy, Destrin, DNA methylation, β-catenin, biomarker

Posted Date: September 29th, 2022

DOI: https://doi.org/10.21203/rs.3.rs-2084750/v1

Abstract

Background

Although surgical resection combined with neoadjuvant radiotherapy can reduce the local recurrence rate of rectal cancer, only some patients benefit from neoadjuvant radiotherapy. Therefore, how to screen out rectal cancer patients who are sensitive or resistant to radiotherapy has great clinical significance.

Results

We found that *DSTN* was highly expressed (P <0.05) and hypomethylated (P <0.01) in neoadjuvant radiotherapy resistant tissues of rectal cancer. Follow-up data confirmed that patients with high expression of *DSTN* in neoadjuvant radiotherapy resistant tissues of rectal cancer had a shorter disease-free survival (P <0.05). *DSTN* expression increased after methyltransferase inhibitor inhibited DNA methylation in DNA promoter region of colorectal cancer cells (P <0.05). In vitro and in vivo experiments showed that knockdown of *DSTN* could promote the sensitivity of colorectal cancer cells to radiotherapy, and overexpression of *DSTN* could promote the resistance of colorectal cancer cells to radiation (P <0.05). The expression of C-Myc and Cyclin D1, which are downstream of Wnt/β-catenin signaling pathway, were up-regulated in colorectal cancer cells with overexpression of *DSTN*. The expression of β-catenin was highly expressed in radiotherapy resistant tissues, and there was a linear correlation between the expression of *DSTN* and β-catenin (P <0.0001). Further studies showed that *DSTN* could bind to β-catenin and increase the stability of β-catenin.

Conclusion

The degree of DNA methylation and the expression level of *DSTN* can be used as a biomarker to predict the sensitivity of neoadjuvant radiotherapy for rectal cancer, and *DSTN* and β-catenin are also expected to become a reference and a new target for the selection of neoadjuvant radiotherapy for rectal cancer.

Introduction

Colorectal cancer (CRC) is one of the most common malignant tumors[1]. There are still some differences in the composition of CRC between the East and the West[2]. China has a higher incidence of rectal cancer (RC) and a higher proportion of low RC[3]. At present, surgical resection is one of the most important treatment methods for RC[4], but there are still some problems such as high local recurrence rate and difficulty in anal preservation in low RC. With the improvement of surgical techniques and the addition of neoadjuvant radiotherapy, the 5-year local recurrence rate decreased from > 25% to approximately 5–10%[5–9]. Neoadjuvant radiotherapy is a treatment method specific to RC, which can effectively reduce the local recurrence rate[10]. For some patients, the range of surgical resection can be reduced due to tumor partial regression, local resection can replace radical surgery; patients with clinical complete response even do not need surgery, so as to improve the sphincter preservation rate of patients with RC[11–15]. However, neoadjuvant radiotherapy for RC is also a double-edged sword. Only part of patients can benefit from neoadjuvant radiotherapy, the remaining patients who are not sensitive to radiotherapy may delay the timing of surgical treatment, thus resulting in distant metastasis[16–18]. In addition, the side effects of radiotherapy such as anus dysfunction and radioactive enteritis have a great impact on patients' quality of life[19, 20]. Current neoadjuvant radiotherapy lacks specificity that it treats potential sensitive/resistant patients with the same treatment strategy[21, 22]. Therefore, how to screen out RC patients who are sensitive or resistant to radiotherapy has great clinical significance.

DNA methylation refers to the chemical modification process in which a specific base on DNA sequence obtains a methyl group by covalent bonding with S-adenosine methionine (SAM) under the catalytic action of DNA methyltransferase (DNMT)[23]. DNA methylation involved in general studies mainly refers to the methylation process of the 5th carbon atom on cytosine in CpG dinucleotide, and its product is called 5-methylcytosine (5-MC). Clusters of CpG dinucleotides within the human genome are called CpG islands. CpG islands are generally located in the promoter region of genes and contain binding sites for many transcription factors. Methylation in this region is often closely related to gene transcription. DNA methylation is a relatively stable modification state. Under the action of DNA methyltransferase, DNA methyltransferase can be inherited to newborn progeny DNA along with the replication process of DNA, which is an important epigenetic mechanism[24, 25]. Here we combined DNA methylation and proteomics in order to explore the key factors affecting radiotherapy sensitivity in RC.

DSTN (Destrin, Actin Depolymerizing Factor) is a Protein Coding gene. The product of this gene belongs to the actin-binding proteins ADF family. This family of proteins is responsible for enhancing the turnover rate of actin *in vivo*. This gene encodes the actin depolymerizing protein that severs actin filaments (F-actin) and binds to actin monomers (G-actin). Two transcript variants encoding distinct isoforms have been identified for this gene. In this study, we found DNA methylation and expression of *DSTN* was related to radiation sensitivity of RC and explored its function and mechanism.

Results

DNA methylation levels of DSTN were reduced and DSTN expression was increased in the radiation-resistant tissues of RC.

In order to explore the relation between DNA methylation and radiation sensitivity, we selected radiation-sensitive and radiation-resistant biopsy tissues for Illumina Human Methylation 850K microarray (Table S1, Fig. 1a). According to the diffscore and delta-beta values, as well as the differential methylated sites located in the promoter region, a total of 24644 differential methylated sites were screened out. Combining the above differential methylated sites with quantitative proteomics data of 70 biopsy tissues before neoadjuvant radiotherapy (unpublished data), a total of 18 differential genes were screened. The screening process was shown in Fig. 1b and the protein expression of 18 genes was shown in Fig. 1c. We selected *DSTN*, *DCN*, *RECK* and *DSG3*, a total of 4 genes that have been reported to be closely related in the process of tumor occurrence and development. We found that mRNA expression of *DSTN* was significantly higher in radiation-resistant biopsy tissues of RC with qRT-PCR (Table S2, Fig. 1d). The methylation level of *DSTN* was validated higher in

radiation-sensitive biopsy tissues of RC with Agena MassARRAY Methylation (Table S3, Fig. 1e). We further used IHC to confirm that the protein expression of *DSTN* was higher in radiation-resistant surgical tissues of RC and the high expression of *DSTN* was related to poor DFS (Table S4, Fig. 1f-g).

Thus, we found that the DNA methylation level of *DSTN* was lower and the mRNA and protein expression of *DSTN* was higher in radiation-resistant tissues of RC.

Reducing the methylation levels of the DSTN **by decitabine in RC cells could increase the expression of** DSTN.

To find the relation between the DNA methylation and expression of *DSTN*, we adopted the CRC cell lines to further validation. The mRNA expression of *DSTN* in CRC cells was higher than in FHC, and the mRNA expression of *DSTN* in HT29 cells was highest in CRC cells, on the contrary, the mRNA expression of *DSTN* in HCT116 cells was lowest in CRC cells (Fig. 2a). CCK-8 assay was used to identify that the optimal radiation dose for HCT116 was 8Gy and for HT29 was 10Gy (Fig. 2b). To determine whether methylation changes affected its expression, we treated the CRC cell lines with decitabine, which is a specific inhibitor of DNA methylation transferase and can reverse DNA methylation process, and found the up-regulation of *DSTN* expression (Fig. 2c). We also detected a higher methylation of *DSTN* in HCT116 cells after radiation by Agena MassARRAY Methylation and the protein expression of *DSTN* was accordingly down-regulated by western blot, while the changes were not observed in HT29 cells (Fig. 2d-e).

Downregulation of DSTN **could promote the sensitivity of RC cells to radiation.**

To further research the function of *DSTN* in radiation resistance, we suppressed *DSTN* expression utilizing two small interfering RNAs (siRNAs) against *DSTN* in the HT29 cell lines (Fig. 3a). Compared to the control group, silencing *DSTN* led to decreased IC50 values in HT29 cells (Fig. 3b) as well as a decreased capacity for cloning after radiation (Fig. 3c). Consistently, flow cytometry showed that an exposure to radiation resulted in an increased proportion of apoptotic cells among *DSTN*-knockdown HT29 cells (Fig. 3d). Together, these data indicate that *DSTN* was required for radiation resistance *in vitro*.

Overexpression of DSTN **could promote radiation resistance in RC** in vitro **and** in vivo.

Next, we overexpressed *DSTN* in the HCT116 cell lines (Fig. 4a). Compared with the control group, HCT116C cells overexpressing *DSTN* displayed an increased tolerance to radiation and led to increased IC50 values (Fig. 4b). Meanwhile, the capacity for cloning was also enhanced after radiation (Fig. 4c). Flow cytometry also showed that *DSTN* overexpression attenuated radiation-induced cell apoptosis (Fig. 4d).

Then, we injected *DSTN*-overexpressing and control HCT116 cells subcutaneously into one side of groin in nude mice and the nude mice were treated with radiation. The results showed that the xenografts formed from *DSTN*-overexpressing RCC cells exhibited worse responses to radiation (Fig. 4e).

Above all, these findings indicate that the overexpression of *DSTN* endowed CRC cells with resistance to radiation.

DSTN **could bind with β-Catenin and activate Wnt/β-Catenin signaling pathway.**

To illuminate the mechanism underlying the role of *DSTN* in radiation resistance of RC, we researched the articles and found the expression of *DSTN* was related to the expression of β-Catenin. We validated that the protein expression of β-Catenin was up-regulated accordingly with the up-regulation of *DSTN* (Fig. 5a). Next, we detected the targeted proteins in Wnt/β-Catenin signaling pathway and found the expressions of β-Catenin, C-Myc and Cyclin D1 was up-regulated too (Fig. 5b). However, the mRNA expression of β-Catenin was not changed with the up-regulation of *DSTN* (Fig. 5c). We supposed that there were interactions between proteins and β-Catenin was shown to be able to combine with *DSTN* by Co-IP (Fig. 5d). IF also validated that *DSTN* and β-Catenin had co-location (Fig. 5e).

DSTN **is linear correlated to β-Catenin and could promote the stability of β-Catenin after radiation.**

We used a tissue microarray to detect the expression of β-Catenin by IHC and found that β-Catenin was upregulated in the radiation-resistant tissues of RC and the expression of β-Catenin was linear correlated to *DSTN* (Fig. 6a-c). To further investigate whether *DSTN* could inhibit the degradation of β-Catenin, a cycloheximide (CHX) chase experiment was performed. The results of this experiment demonstrated that the overexpression of *DSTN* could increase the stability of β-Catenin (Fig. 6d).

Discussion

DNA methylation can be involved in regulating gene expression and is closely related to many physiological and pathological processes such as the occurrence and development of a variety of tumors[26–28], embryonic development[29, 30], aging[31, 32], and can be used as a marker for diagnosis, prognosis and treatment of many diseases[33–38].Currently, DNA methylation has been shown to play a role in radiation therapy, Laura P Sutton et al found that methyltransferase inhibitors can delay the phosphorylation of BRCA1 and the repair of double chain break, thus affecting the response to radiotherapy in prostate cancer[39]. Christoph Weigel et al showed that DNA methylation of DKGA can promote radiation-induced fibrosis in breast cancer[40], K Yokoi et al. found that methylation of CRBP1 promoter region affects radiotherapy sensitivity of CRC cell lines[41]. However, there is still a lack of systematic and in-depth research on the effect of DNA methylation regarding neoadjuvant radiotherapy in patients with RC. In this study, through combining the results of DNA methylation and proteomics, we found *DSTN* hypomethylation and high expression in radiation-resistant tissues. The above results were validated by Agena Methylation, qRT-PCR and IHC. The survival analysis also showed that high expression of *DSTN* was related to poor DFS.

DSTN encodes destrin, a member of the actin binding protein family, which is responsible for increasing turnover rate of actin *in vivo*[42]. Destrin is involved in the precise regulation of cytoskeleton remodeling and actin filament turnover, as well as many cellular processes such as cell division, proliferation and membrane transport[43, 44]. Studies have shown that actin dynamics and its regulation of target proteins are not only important for healthy cell development

and function, but also play a crucial role in cancer and other diseases. Recent studies have found that *DSTN* is associated with multiple cancers, such as gastric cancer[45] and liver metastasis of lung cancer[46]. In this study, we constructed the *DSTN* knockdown and overexpression CRC cells in order to observe the function changes after radiation *in vitro* and *vivo* through CCK 8 multiplication experiment, clone formation, and flowcytometry. *In vitro* experiments we found down-regulated of *DSTN* can promote CRC cells sensitivity to radiotherapy, up-regulated of *DSTN* can promote CRC cells to radiation resistance. *In vivo* experiments showed CRC cells with up-regulated of *DSTN* in nude mice after radiation grew faster than the control group, presenting *DSTN* can result in CRC cell with radiation resistance. In addition, after inhibiting the methylation of the *DSTN* promoter region by Decitabine, the expression of *DSTN* was increased, indicating that the change of *DSTN* methylation could affect the expression of *DSTN*.

It has been reported that *DSTN* is associated with β-catenin and can activate Wnt/β-catenin pathway and EMT pathway to promote liver metastasis of lung cancer[46]. β-catenin are part of the protein complex that makes up cell adhesion, and also anchor the actin cytoskeleton, transmitting contact inhibition signals that cause cells to stop dividing[47, 48]. β-catenin gene mutations are one of the etiologies of CRC, liver cancer, hairy blastoma, medulloblastoma and ovarian cancer[49–51]. Here, we found activation of Wnt/β-catenin signaling pathway in CRC cells with stable overexpression of *DSTN*, and downstream pathway expressions of C-Myc and Cyclin D1 were up-regulated. The binding of *DSTN* to β-catenin was confirmed by CO-IP and IF. Next, we validated that β-catenin was highly expressed in radiotherapy resistant tissues, and there was a linear correlation with *DSTN* expression. By adding CHX, we found that *DSTN* binding to β-catenin could increase the stability of β-catenin.

In conclusion, we showed that *DSTN*, which is regulated by DNA methylation, promoted radiotherapy resistance by increasing the stability of β-catenin and activating Wnt/β-catenin signaling pathway in RC.

Materials And Methods

RC patients and clinical samples

All RC tissue samples involved in the study were obtained from Changhai Hospital, which had signed informed consent and been approved by the Ethics Committee of Changhai Hospital. RC specimens used in this study were biopsy tissues before neoadjuvant radiotherapy or surgically resected specimens after neoadjuvant radiotherapy in the Department of Colorectal Surgery. Tumor regression grade (TRG) was obtained to evaluate the response of neoadjuvant radiotherapy[52]. Inclusion criteria: 1. Pathological diagnosis of RC; 2. Aged between 18 and 75; 3. Neoadjuvant radiotherapy was performed in Changhai Hospital. Exclusion criteria: 1. Withdrawal during neoadjuvant radiotherapy; 2. No operation was performed after neoadjuvant radiotherapy; 3. There was no TRG score in pathology. Five pairs of radiation-sensitive (TRG0) and resistant (TRG3) RC biopsy tissues were used for Illumina Human Methylation 850K microarray (Table S1). Ten pairs of radiation-sensitive (TRG0-1) and resistant (TRG2-3) RC biopsy tissues were used for mRNA expression detection (Table S2). Another ten pairs of radiation-sensitive (TRG0-1) and resistant (TRG2-3) RC biopsy tissues were used for Agena MassARRAY Methylation verification (Table S3). Surgical specimens of 68 RC patients after neoadjuvant radiotherapy were collected to construct a tissue microarray and detect the expression of *DSTN* by IHC (Table S4).

Illumina Human Methylation 850K microarray

The 850K microarray can detect the methylation status of about 853,307 CpG sites in the whole human genome, including 91% of the original 450K microarray sites, and an increase of 413,745 sites. The 850K microarray not only maintains the comprehensive coverage of CpG island, gene promoter region, but also specially increases the probe coverage of the enhancer region and gene coding region. Illumina Human Methylation 850K microarray detection and data analysis were performed by Genergy (Shanghai).

Agena MassARRAY methylation

The Agena MassARRAY Methylation process includes bisulfite conversion, PCR amplification, *in vitro* transcription and RNase A-specific digestion, and matriX-assisted laser desorption/ionization-time of flight. Agena MassARRAY methylation detection and data analysis were performed by CapitalBio Technology Corporation (Beijing).

Proteomics

The process of proteomics includes protein or peptide fluorescence quantification, filter-aided sample preparation, tandem mass tag, peptide stage tip desalination, classification of inverted peptides, and multi-dimensional liquid chromatography with mass spectrometry analysis. Proteomics detection and data analysis were performed by Shanghai Academy of Biological Sciences, Chinese Academy of Sciences.

Cell Lines and reagents

The human CRC cell lines (HCT116, HT29, SW480, SW620, CACO2) and FHC cells were obtained from the Chinese Academy of Sciences (Shanghai, China). Cells were incubated in Dulbecco's Modified Eagle Medium (DMEM) (SH30022.01, HyClone, USA) supplemented with 10% foetal bovine serum (FBS, 10099141, Gibco, USA). Decitabine were purchased from Selleck Chemicals (China). Cycloheximide (CHX) were purchased from APExBIO (USA).

Animal studies

The animal studies were approved by the Institutional Animal Care and Use Committee of the Second Military Medical University, Shanghai, China. Male athymic BALB/c nude mice (5 weeks old) were used. A total of 5×10^6 lv-*DSTN* cells were injected subcutaneously into one side of groin (n=3). When the xenografts grew to 100 mm^3, simulated radiotherapy was started (a total of 20Gy radiation and control). Xenograft volumes were evaluated by caliper

measurements and calculated individually with the following formula: Volume = a×b^2/2 (where a represents the longest diameter and b represents the shortest diameter). Xenograft volumes was measured every 3 days and xenograft growth curve was drawn for 30 days in total.

RNA extraction, cDNA preparation and qRT -PCR

Total RNA was extracted from cells and tissues with TRIzol reagents (Takara, Japan), and the quality of RNA was determined with a Nanodrop 2000 and agarose gel electrophoresis. First-strand cDNA was generated from total RNA with PrimeScript™ RT Master Mix (Takara, Japan). qRT-PCR was performed with TB Green Premix Ex Taq (Takara, Japan) in a Step One Plus System (Applied Biosystems, USA), and β-actin served as the endogenous control. The primer sequences used were as follows: *DSTN*, 5'-GCTGATGAAGTATGTCGCATTT-3' (forward) and 5'-CGACAATCTTTTTCAGGAAGCA-3'

(reverse); *DSG3*, 5'-TAAAGACAGCGGTTATGGGATT-3' (forward) and 5'-CTGACAAAGTCTGGCACTTAAC-3' (reverse); *DCN*, 5'-GACAACAACAAGCTTACCAGAG-3' (forward) and 5'-TGAAAAGACTCACACCCGAATA-3' (reverse); *RECK*, 5'-GCACAACAATCTCTGCACTTTA-3' (forward) and 5'-CAGTCCCCATAGTAATCGACTG-3' (reverse); β-catenin, 5'-TGGATTGATTCGAAATCTTGCC-3' (forward) and 5'-GAACAAGCAACTGAACTAGTCG-3' (reverse) and β-actin, 5'-GGGCACGAAGGCTCATCATT-3' (forward) and 5'-AGCGAGCATCCCCCAAAGTT-3' (reverse). Relative mRNA expression levels were calculated based on the corresponding relative quantitation (RQ) values and were normalized to β-actin expression.

Western blot analysis

Protein was extracted from cells and tissues with lysis buffer, protease inhibitor mixture, loading buffer according to the manufacturer's instructions (Beyotime, China). Then the protein went through gel electrophoresis and transferred onto polyvinylidene fluoride membranes. After incubating with primary and secondary antibodies, the bands were detected through Odyssey infrared scanner (Li-Cor). The primary antibodies included against *DSTN* (ab186754, Abcam, USA), β-catenin (51067-2-AP, Proteintech, China), C-Myc (10828-1-AP, Proteintech, China), Cyclin D1 (60186-1-Ig, Proteintech, China) and β-actin (66009-1-Ig, Proteintech, China) for control. The secondary antibodies included goat anti-mouse IgG (A327300, Thermo Fisher Scientific, USA) and goat anti-rabbit IgG (A32734, Thermo Fisher Scientific, USA).

siRNA transfection

The CRC cells were inoculated into a six-well plate, and when the cell density reached about 50%, the transfection reagent was added according to the manufacturer's instructions for lipofectamine 3000 (Thermo Fisher Scientific, USA). *DSTN* siRNA was synthesized by GenePharma (Shanghai, China), with the following sequences: 5'-GCUGAUGAAGUAUGUCGCATT-3' (forward) and 5'-UGCGACAUACUUCAUCAGCTT-3' (reverse); and 5'-UCAAGCAAAUGGACCAGAATT-3' (forward) and 5'-UUCUGGUCCAUUUGCUUGATT-3' (reverse). A non-silencing siRNA oligonucleotide that does not recognize any known mammalian gene homologue (GenePharma, Shanghai, China) was used as the negative control, with the following sequence: 5'-UUCUCCGAACGUGUCACGUTT-3' (forward) and 5'-ACGUGACACGUUCGGAGAATT-3' (reverse).

Lentiviral packaging and transfection

The lentivirus with stable overexpression of *DSTN* was constructed by GenePharma (Shanghai, China), where the overexpression sequence is ATGGCCTCAGGAGTGCAAGTAGCTGATGAAGTATGTCGCAT
TTTTTATGACATGAAAGTTCGTAAATGCTCCACACCAGAAGAAATCAAGAAAAGAAAGAAGGCTGTCATTTTTTGTCTCAGTGCAGACAAAAAGTGCATCATTGTAGAAG
Infection was performed following the manufacturer's instructions and fluorescence of lentivirus was observed 72h after infection.

Cell counting kit 8 (CCK-8) assay

The cells were inoculated into 96-well plates containing 10μl of CCK-8 reagent and radiated with different doses (0Gy, 2Gy, 4Gy, 8Gy, 10Gy, 16Gy, 20Gy). The optical density (OD) value at 450nm was measured with a microplate reader. Then the dose-response curve of CRC cells to radiation was drawn and half maximal inhibitory concentration (IC50) was calculated.

Plate colony formation assay

CRC cells were inoculated in 6-well plates with 1000 cells per well the day before radiation. After 10 days, the 6-well plate was washed twice with PBS, fixed with 4% paraformaldehyde for 1h, stained with crystal violet for 1h, cleaned with PBS, dried and photographed, and the number of clones was calculated.

Flow cytometric analysis

Cell apoptosis was quantified using flow cytometric analysis (BD Biosciences, San Jose, CA). For apoptosis experiments, CRC cells after radiation were collected and washed twice with ice-cold PBS and then re-suspended in 200μl of binding buffer. Fluorescein isothiocyanate (FITC)-conjugated Annexin V was added at a final concentration of 0.5μg/ml and incubated for 20 minutes at room temperature in the dark; then, 1μg/ml propidium iodide (PI) was added. The samples were immediately analyzed by flow cytometry.

Co-immunoprecipitation

Co-immunoprecipitation (co-IP) was performed according to the manufacturer's instructions (KIP-1, Proteintech). Antibodies against *DSTN* (ab186754, Abcam, 1:50) and β-catenin (51067-2-AP, Proteintech, 1:30) were used.

Immunofluorescence (IF)

The cells were inoculated in a 6-well plate containing slides the day before radiation. The medium was removed and the plate was cleaned with PBS 48h after radiation. The cells were fixed with 4% paraformaldehyde for 30min, then the paraformaldehyde was discarded and the plate was washed with PBS for 3 times. The follow-up experiment was completed by Servicebio (Shanghai, China). Representative images were acquired using the Leica Microsystem. DAPI glows blue by UV excitation wavelength 330-380 nm and emission wavelength 420 nm; FITC glows green by excitation wavelength 465-495 nm and emission wavelength 515-555 nm; CY3 glows red by excitation wavelength 510-560 nm and emission wavelength 590 nm. Nucleus is blue by labeling with DAPI, *DSTN* is green by labeling with FITC and β-catenin is red by labeling with CY3. After merging under the microscope, the yellow fluorescence indicates co-localization of *DSTN* and β-catenin.

Immunohistochemistry (IHC)

Specimens were stained with antibodies for *DSTN* (ab186754, 1:100) or β-catenin (51067-2-AP, 1:100). The follow-up experiment of IHC was completed by Servicebio (Shanghai, China). Staining intensities and percentages of positive tumour cells was automatically calculated using the Servicebio image analysis system.

Data analysis

All statistical analyses in this study were performed with SPSS 26.0 software (SPSS Inc, USA). The measurement data were expressed as means±sd, and a two-tailed Student's t test was used for comparison between groups. Spearman correlation analysis was performed to determine the correlation between two variables. Kaplan-meier method was used to draw disease free survival (DFS) curve and overall survival (OS) curve, and log-rank test was used for survival analysis. A p-value less than 0.05 was considered significant.

Declarations

Funding

National Natural Science Foundation of China(82072750), Natural Science Fund of Shanghai(20ZR1457200), Shanghai Sailing Program(21YF1459300), The 71st Batch of China Postdoctoral Science Foundation (48804)

Ethical Approval and consent to participate

The experimental protocol was approved by Shanghai Changhai Hospital Ethics Committee.

Patient consent for publication

Not required.

Competing interests

Authors declare that they have no competing interests.

Author Contributions

W.Z., F.Y and G.Y. designed the study and drafted the manuscript. R.W., L.Z., S.J., and H.F prepared the tables and figures and drafted the manuscript., K.Z., and Y.Y. contributed to the clinical sample collection. X.G., Z.L. and L.H. contributed to the editing and review. All authors participated in revising the manuscript. All authors contributed to the article and approved the submitted version.

Availability of data and materials

All datasets presented in this study are included in the article/supplementary material.

Acknowledgments

The authors thanks the National Natural Science Foundation of China(82072750), Natural Science Fund of Shanghai(20ZR1457200), Shanghai Sailing Program(21YF1459300) and The 71st Batch of China Postdoctoral Science Foundation (48804) for the funding of this study.

References

1. Siegel RL, Miller KD, Goding Sauer A et al. Colorectal cancer statistics, 2020. CA Cancer J Clin. 2020, 70(3):145–164.
2. Deng Y. Rectal Cancer in Asian vs. Western Countries: Why the Variation in Incidence? Curr Treat Options Oncol. 2017, 18(10):64.
3. Sung JJY, Chiu HM, Jung KW et al. Increasing Trend in Young-Onset Colorectal Cancer in Asia: More Cancers in Men and More Rectal Cancers. Am J Gastroenterol. 2019, 114(2):322–329.
4. MacFarlane JK, Ryall RD, Heald RJ. Mesorectal excision for rectal cancer. Lancet. 1993, 341(8843):457–460.
5. Swedish Rectal Cancer T, Cedermark B, Dahlberg M et al. Improved survival with preoperative radiotherapy in resectable rectal cancer. N Engl J Med. 1997, 336(14):980–987.
6. Sauer R, Becker H, Hohenberger W et al. Preoperative versus postoperative chemoradiotherapy for rectal cancer. N Engl J Med. 2004, 351(17):1731–1740.

7. Bosset JF, Collette L, Calais G et al. Chemotherapy with preoperative radiotherapy in rectal cancer. N Engl J Med. 2006, 355(11):1114–1123.
8. Peeters KC, Marijnen CA, Nagtegaal ID et al. The TME trial after a median follow-up of 6 years: increased local control but no survival benefit in irradiated patients with resectable rectal carcinoma. Ann Surg. 2007, 246(5):693–701.
9. Sebag-Montefiore D, Stephens RJ, Steele R et al. Preoperative radiotherapy versus selective postoperative chemoradiotherapy in patients with rectal cancer (MRC CR07 and NCIC-CTG C016): a multicentre, randomised trial. Lancet. 2009, 373(9666):811–820.
10. Maas M, Beets-Tan RG, Lambregts DM et al. Wait-and-see policy for clinical complete responders after chemoradiation for rectal cancer. J Clin Oncol. 2011, 29(35):4633–4640.
11. Callender GG, Das P, Rodriguez-Bigas MA et al. Local excision after preoperative chemoradiation results in an equivalent outcome to total mesorectal excision in selected patients with T3 rectal cancer. Ann Surg Oncol. 2010, 17(2):441–447.
12. Cao B, Min L, Zhu S, Shi H, Zhang S. Long-term oncological outcomes of local excision versus radical resection for early colorectal cancer in young patients without preoperative chemoradiotherapy: a population-based propensity matching study. Cancer Med. 2018, 7(6):2415–2422.
13. Wang T, Wang J, Deng Y, Wu X, Wang L. Neoadjuvant therapy followed by local excision and two-stage total mesorectal excision: a new strategy for sphincter preservation in locally advanced ultra-low rectal cancer. Gastroenterol Rep (Oxf). 2014, 2(1):37–43.
14. Habr-Gama A, Sabbaga J, Gama-Rodrigues J et al. Watch and wait approach following extended neoadjuvant chemoradiation for distal rectal cancer: are we getting closer to anal cancer management? Dis Colon Rectum. 2013, 56(10):1109–1117.
15. Lai CL, Lai MJ, Wu CC, Jao SW, Hsiao CW. Rectal cancer with complete clinical response after neoadjuvant chemoradiotherapy, surgery, or "watch and wait". Int J Colorectal Dis. 2016, 31(2):413–419.
16. Tuta M, Boc N, Brecelj E, Peternel M, Velenik V. Total neoadjuvant therapy vs standard therapy of locally advanced rectal cancer with high-risk factors for failure. World J Gastrointest Oncol. 2021, 13(2):119–130.
17. Mroczkowski P, Dziki L. Total neoadjuvant therapy in rectal cancer - improvement or overtreatment? Br J Surg. 2019, 106(11):1558.
18. Parmar KL, Malcomson L, Renehan AG. Watch and wait or surgery for clinical complete response in rectal cancer: a need to study both sides. Colorectal Dis. 2020, 22(7):839–840.
19. van der Sande ME, Hupkens BJP, Berbee M et al. Impact of radiotherapy on anorectal function in patients with rectal cancer following a watch and wait programme. Radiother Oncol. 2019, 132:79–84.
20. Quezada-Diaz F, Jimenez-Rodriguez RM, Pappou EP et al. Effect of Neoadjuvant Systemic Chemotherapy With or Without Chemoradiation on Bowel Function in Rectal Cancer Patients Treated With Total Mesorectal Excision. J Gastrointest Surg. 2019, 23(4):800–807.
21. Benson AB, Venook AP, Al-Hawary MM et al. Rectal Cancer, Version 2.2018, NCCN Clinical Practice Guidelines in Oncology. J Natl Compr Canc Netw. 2018, 16(7):874–901.
22. Glynne-Jones R, Wyrwicz L, Tiret E et al. Rectal cancer: ESMO Clinical Practice Guidelines for diagnosis, treatment and follow-up. Ann Oncol. 2018, 29(Suppl 4):iv263.
23. Meier K, Recillas-Targa F. New insights on the role of DNA methylation from a global view. Front Biosci (Landmark Ed). 2017, 22(4):644–668.
24. Meng H, Cao Y, Qin J et al. DNA methylation, its mediators and genome integrity. Int J Biol Sci. 2015, 11(5):604–617.
25. Marchal C, Miotto B. Emerging concept in DNA methylation: role of transcription factors in shaping DNA methylation patterns. J Cell Physiol. 2015, 230(4):743–751.
26. Lasseigne BN, Brooks JD. The Role of DNA Methylation in Renal Cell Carcinoma. Mol Diagn Ther. 2018, 22(4):431–442.
27. Pfeifer GP. Defining Driver DNA Methylation Changes in Human Cancer. Int J Mol Sci. 2018, 19(4).
28. Sui J, Wu X, Wang C et al. Discovery and validation of methylation signatures in blood-based circulating tumor cell-free DNA in early detection of colorectal carcinoma: a case-control study. Clin Epigenetics. 2021, 13(1):26.
29. Elhamamsy AR. Role of DNA methylation in imprinting disorders: an updated review. J Assist Reprod Genet. 2017, 34(5):549–562.
30. Breton-Larrivee M, Elder E, McGraw S. DNA methylation, environmental exposures and early embryo development. Anim Reprod. 2019, 16(3):465–474.
31. Jones MJ, Goodman SJ, Kobor MS. DNA methylation and healthy human aging. Aging Cell. 2015, 14(6):924–932.
32. Xiao FH, Kong QP, Perry B, He YH. Progress on the role of DNA methylation in aging and longevity. Brief Funct Genomics. 2016, 15(6):454–459.
33. Pan Y, Liu G, Zhou F, Su B, Li Y. DNA methylation profiles in cancer diagnosis and therapeutics. Clin Exp Med. 2018, 18(1):1–14.
34. Zhu H, Zhu H, Tian M, Wang D, He J, Xu T. DNA Methylation and Hydroxymethylation in Cervical Cancer: Diagnosis, Prognosis and Treatment. Front Genet. 2020, 11:347.
35. Frontiers Production O. Erratum: A DNA Methylation-Based Panel for the Prognosis and Diagnosis of Patients With Breast Cancer and Its Mechanisms. Front Mol Biosci. 2020, 7:596445.
36. Nikas JB, Nikas EG. Genome-Wide DNA Methylation Model for the Diagnosis of Prostate Cancer. ACS Omega. 2019, 4(12):14895–14901.
37. Li D, Zhang L, Liu Y et al. Specific DNA methylation markers in the diagnosis and prognosis of esophageal cancer. Aging (Albany NY). 2019, 11(23):11640–11658.
38. Mojtabanezhad Shariatpanahi A, Yassi M, Nouraie M, Sahebkar A, Varshoee Tabrizi F, Kerachian MA. The importance of stool DNA methylation in colorectal cancer diagnosis: A meta-analysis. PLoS One. 2018, 13(7):e0200735.
39. Sutton LP, Jeffreys SA, Phillips JL et al. DNA methylation changes following DNA damage in prostate cancer cells. Epigenetics. 2019, 14(10):989–1002.
40. Weigel C, Veldwijk MR, Oakes CC et al. Epigenetic regulation of diacylglycerol kinase alpha promotes radiation-induced fibrosis. Nat Commun. 2016, 7:10893.

41. Yokoi K, Yamashita K, Ishii S et al. Comprehensive molecular exploration identified promoter DNA methylation of the CRBP1 gene as a determinant of radiation sensitivity in rectal cancer. Br J Cancer. 2017, 116(8):1046–1056.
42. Bernstein BW, Bamburg JR. ADF/cofilin: a functional node in cell biology. Trends Cell Biol. 2010, 20(4):187–195.
43. Yamaguchi H, Condeelis J. Regulation of the actin cytoskeleton in cancer cell migration and invasion. Biochim Biophys Acta. 2007, 1773(5):642–652.
44. Le Clainche C, Carlier MF. Regulation of actin assembly associated with protrusion and adhesion in cell migration. Physiol Rev. 2008, 88(2):489–513.
45. Yu J, Liang QY, Wang J et al. Zinc-finger protein 331, a novel putative tumor suppressor, suppresses growth and invasiveness of gastric cancer. Oncogene. 2013, 32(3):307–317.
46. Zhang HJ, Chang WJ, Jia CY et al. Destrin Contributes to Lung Adenocarcinoma Progression by Activating Wnt/beta-Catenin Signaling Pathway. Mol Cancer Res. 2020, 18(12):1789–1802.
47. Valenta T, Hausmann G, Basler K. The many faces and functions of beta-catenin. EMBO J. 2012, 31(12):2714–2736.
48. Pedone E, Marucci L. Role of beta-Catenin Activation Levels and Fluctuations in Controlling Cell Fate. Genes (Basel). 2019, 10(2).
49. Cui C, Zhou X, Zhang W, Qu Y, Ke X. Is beta-Catenin a Druggable Target for Cancer Therapy? Trends Biochem Sci. 2018, 43(8):623–634.
50. Tao J, Zhang R, Singh S et al. Targeting beta-catenin in hepatocellular cancers induced by coexpression of mutant beta-catenin and K-Ras in mice. Hepatology. 2017, 65(5):1581–1599.
51. Sebio A, Kahn M, Lenz HJ. The potential of targeting Wnt/beta-catenin in colon cancer. Expert Opin Ther Targets. 2014, 18(6):611–615.
52. Trakarnsanga A, Gonen M, Shia J et al. Comparison of tumor regression grade systems for locally advanced rectal cancer after multimodality treatment. J Natl Cancer Inst. 2014, 106(10).

Figures

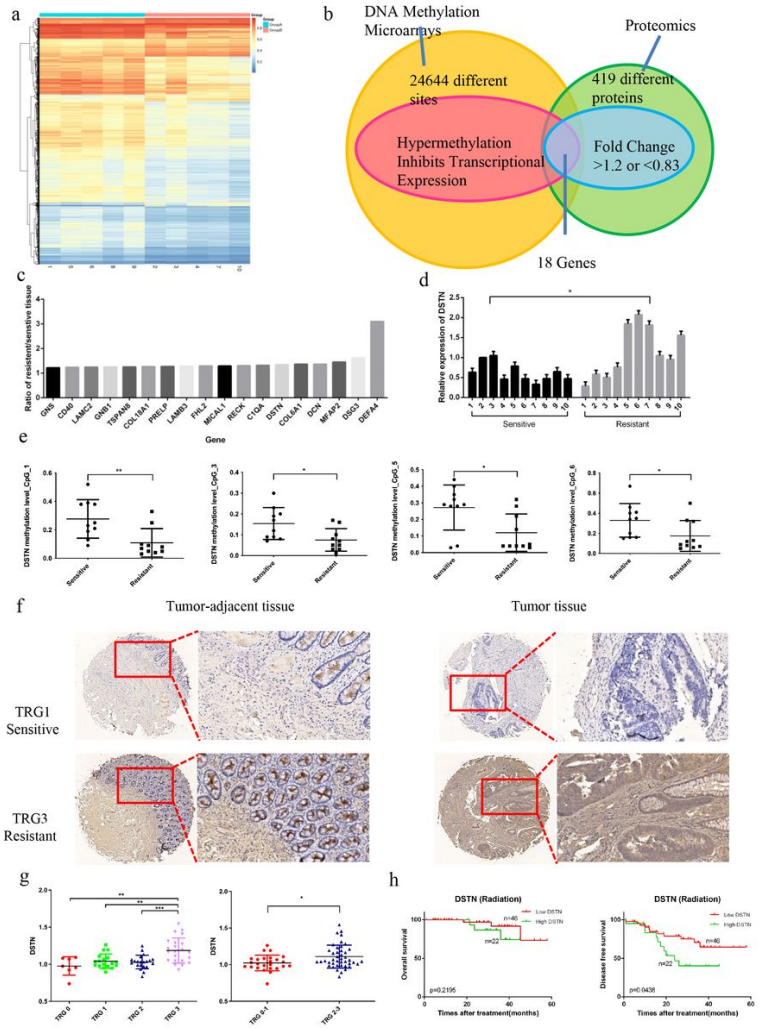

Figure 1

DNA methylation levels of *DSTN* were reduced and *DSTN* expression was increased in the radiation-resistant tissues of RC. (a) Cluster analysis of the Illumina Human Methylation 850K Microarray in 5 pairs of radiation-sensitive and resistant RC tissues (heat map). (b) Methylation 850K microarray and proteomics screening for common differential genes (Screening process). (c) The protein expression level of the 18 screened gene in 70 RC pre-radiotherapy biopsy

tissues by proteomics. (d) mRNA expression of *DSTN* in 10 pairs of radiation-sensitive and resistant RC tissues. (e) CpG sites of *DSTN* that had differences in 10 pairs of radiation-sensitive and resistant RC tissues by Agena MassARRAY Methylation. (f) Representative immunohistochemical results of *DSTN* expression in the radiation-sensitive and resistant tissues of RC, 400X. (g) *DSTN* relative expression (the ratio of tumor tissue to tumor-adjacent tissue) by IHC in RC patients with different TRG scores (n=68, TRG0=7, TRG1=18, TRG2=21, TRG3=22). (h) Kaplan-Meier analysis of OS (left) and DFS (right) in patients according to the expression of *DSTN*. The results are presented as the means ± SD. *p<0.05, **p < 0.01.

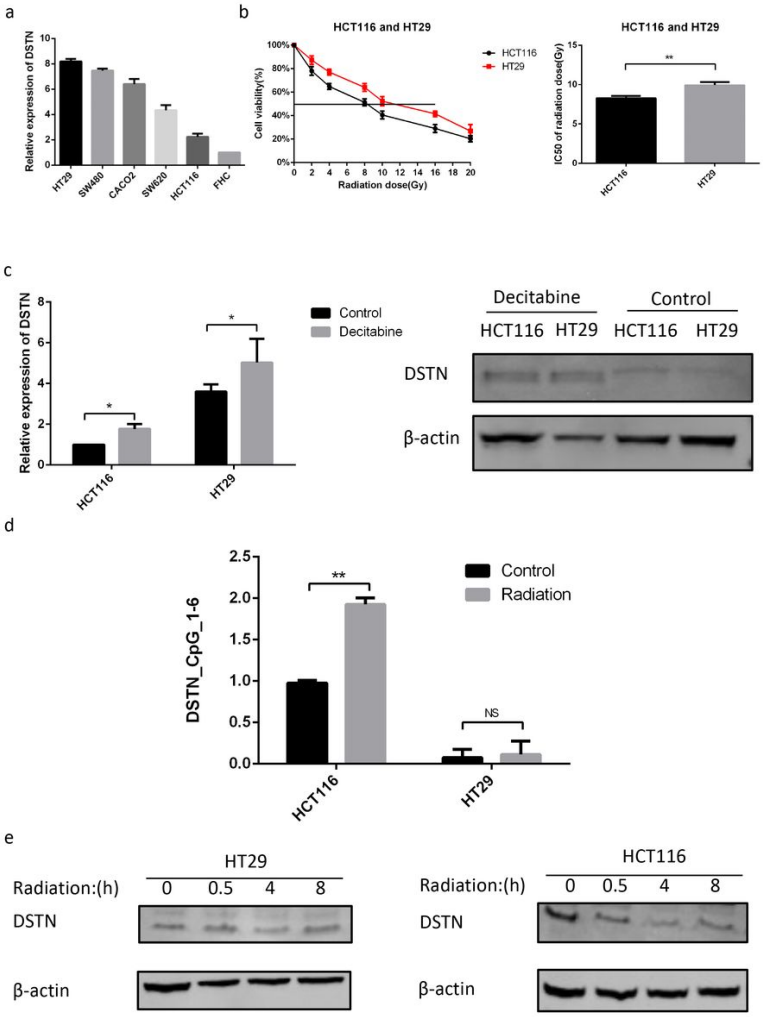

Figure 2

Reducing the methylation levels of the *DSTN* by decitabine in RC cells could increase the expression of *DSTN*. (a) mRNA expression of *DSTN* in RC cell lines and FHC. (b) CCK-8 assay of HCT116 and HT29 cells after radiation at the indicated dose for 48h (n=3). The IC50 values are shown in the right histogram. (c) *DSTN* mRNA (left) and protein (right) expressions were up-regulated by decitabine (2 μM) inhibiting *DSTN* DNA methylation in HCT116 and HT29 cells (n=3). (d) Agena MassARRAY Methylation of *DSTN* in HCT116 and HT29 cells after radiation for 8h and control HCT116 and HT29 cells (n=3). (e) The protein expression levels after different times of radiation in HT29 (10Gy) and HCT116 (8 Gy) cells (n=3). Results are presented as the means ± SD. *p<0.05, **p<0.01, NSp>0.05.

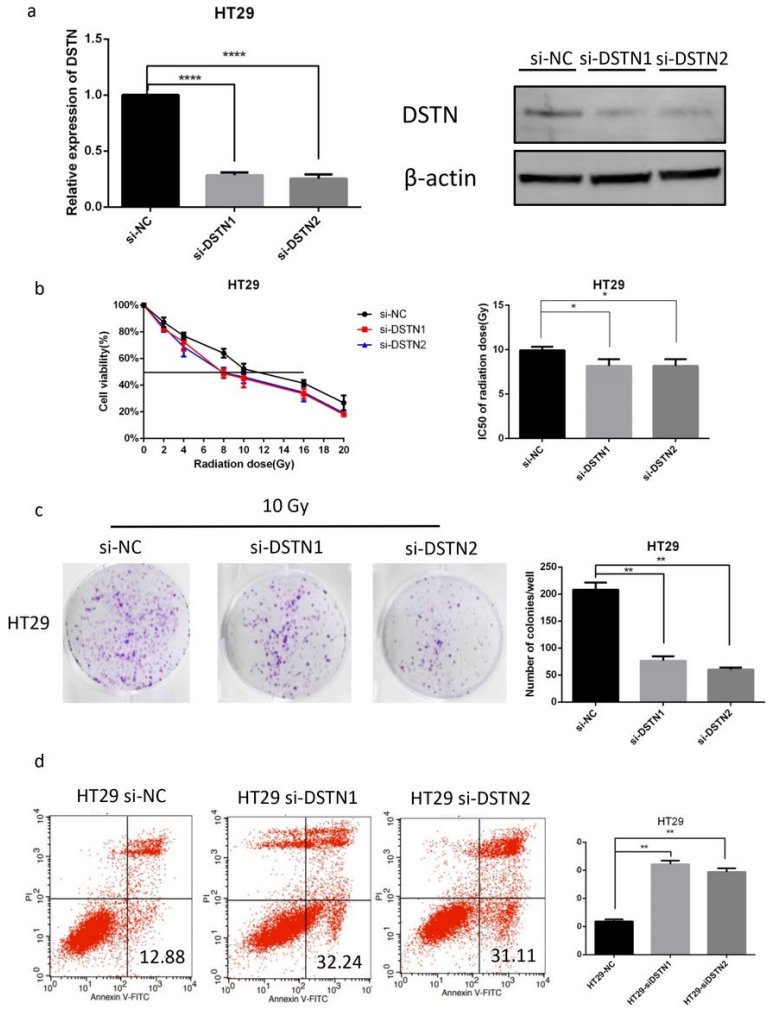

Figure 3

Downregulation of *DSTN* could promote the sensitivity of RC cells to radiation. (a) qPCR (left) and western blot (right) analysis of *DSTN* siRNA interference efficiency in HT29 cells. (b) CCK-8 assay of HT29 cells transfected with si-*DSTN*1, si-*DSTN*2 or si-NC after radiation at the indicated dose for 48h (n=3). The IC50 values are shown in the right histogram. (c) Cell clone formation experiments of HT29 cells transfected with si-*DSTN*1, si-*DSTN*2 or si-NC after radiation (10 Gy) for 10 days (n=3). Representative images (left) and average number of RC colonies (right) are shown. (d) Flow cytometry analysis of Annexin V-stained HT29 cells transfected with si-*DSTN*1, si-*DSTN*2 or si-NC after radiation (10 Gy) for 48 h (n=3). Representative images (left, grids of right side indicate apoptotic cells) and average number of apoptotic cells (right) are shown. Results are presented as the means ± SD. *p<0.05, **p< 0.01, ****p<0.0001.

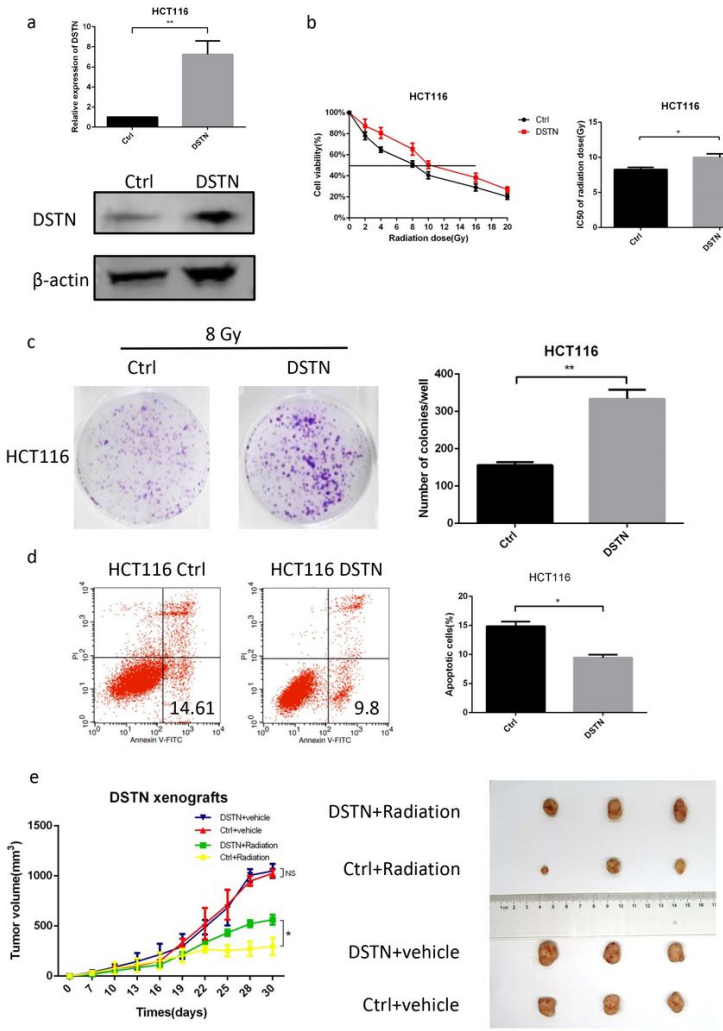

Figure 4

Overexpression of *DSTN* could promote radiation resistance in RC *in vitro* and *in vivo*. (a) qPCR and western blot analysis of lentivirus-*DSTN*overexpression efficiency in HCT116 cells. (b) CCK-8 assay of *DSTN*-overexpressing and control HCT116 cells after radiation at the indicated dose for 48h (n=3). The IC50 values are shown in the right histogram. (c) Cell clone formation experiments of *DSTN*-overexpressing and control HCT116 cells after radiation (8 Gy) for 10 days (n=3). Representative images (left) and average number of RC colonies (right) are shown. (d) Flow cytometry analysis of Annexin V-stained *DSTN*-overexpressing and control HCT116 cells after radiation (8 Gy) for 48 h (n=3). Representative images (left, grids of right side indicate apoptotic cells) and average number of apoptotic cells (right) are shown. (e) Subcutaneous xenograft growth curve in nude mice under different treatment conditions (left) and anatomical picture of subcutaneous xenografts in nude mice (right) are shown. Results are presented as the means ± SD. *p<0.05, **p<0.01, NSp>0.05.

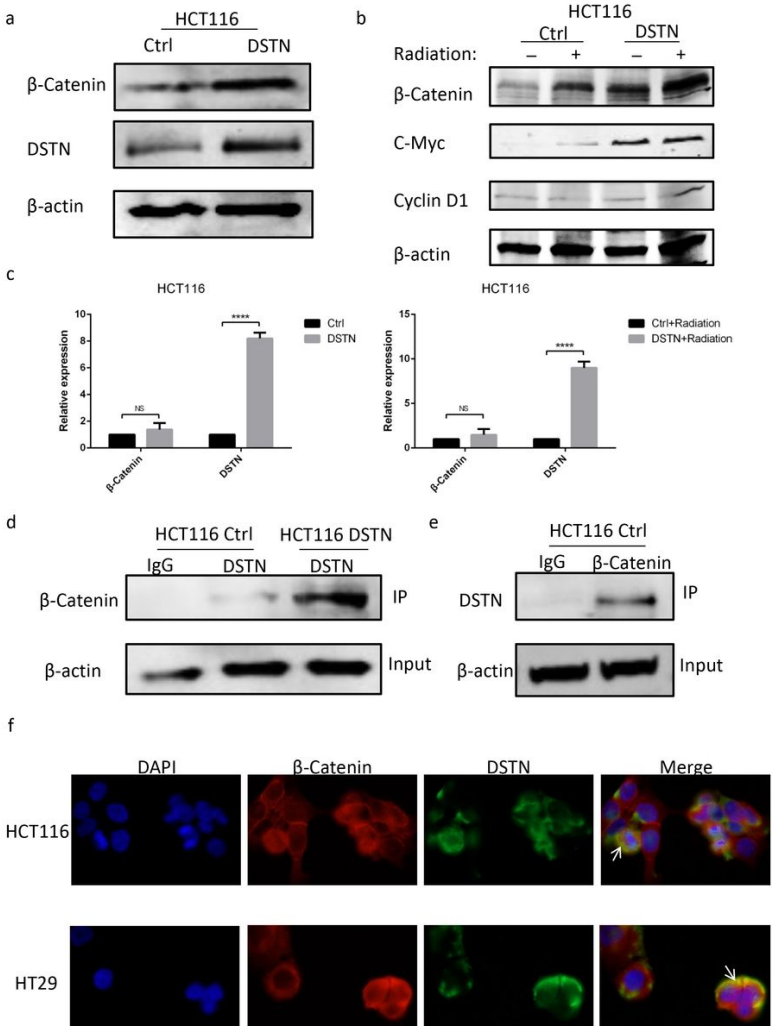

Figure 5

***DSTN* could bind with β-Catenin and activate Wnt/β-Catenin signaling pathway.** (a) Representative images of western blot analysis of *DSTN* and β-Catenin in *DSTN*-overexpressing and control HCT116 cells (n=3). (b) Western blot analysis of Wnt/β-Catenin signaling pathway related β-Catenin, C-Myc, Cyclin D1 in *DSTN*-overexpressing and control HCT116 cells with or without radiation (n=3). (c) mRNA level of β-catenin in *DSTN*-overexpressing and control HCT116 cells with or without radiation (n=3). (d) Co-immunoprecipitation of *DSTN* and β-catenin in HCT116 cells. (e) IF analysis of *DSTN* (green) and β-catenin (red) in HCT116 cells, 400X. The arrow represents co-location. Results are presented as the means ± SD. ****p<0.0001, NSp>0.05.

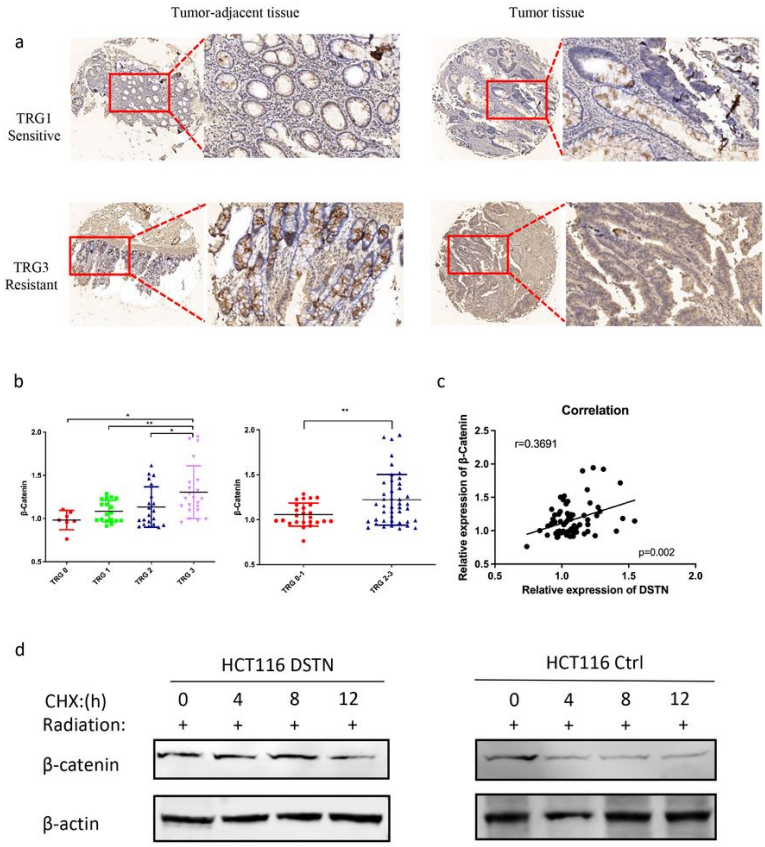

Figure 6

***DSTN* is linear correlated to β-Catenin and could promote the stability of β-Catenin after radiation.** (a) Representative immunohistochemical results of β-catenin expression in the radiation-sensitive and resistant tissues of RC, 400X. (b) β-catenin relative expression (the ratio of tumor tissue to tumor-adjacent tissue) by IHC in RC patients with different TRG scores. (c) Linear correlation between *DSTN*and β-Catenin expression by IHC. (d) Western blot analysis of β-catenin in *DSTN*-overexpressing and control HCT116 cells after cycloheximide (CHX) and radiation (10 Gy) treatment for various times. Results are presented as the means ± SD. *p<0.05.

Supplementary Files

This is a list of supplementary files associated with this preprint. Click to download.

- SupplementTable.xlsx